

Orientational Correlation Function and Persistence Lengths of Flexible Polyelectrolytes

Magnus Ullner^{*,†} and Clifford E. Woodward[‡]

Physical Chemistry 1, Center for Chemistry and Chemical Engineering, Lund University, P.O. Box 124, S-221 00 Lund, Sweden; and School of Chemistry, University College, University of New South Wales, Australian Defence Force Academy, Canberra ACT 2600, Australia

Received May 17, 2001; Revised Manuscript Received October 26, 2001

ABSTRACT: Orientational correlation functions have been obtained from Monte Carlo simulations of long, freely jointed chains (1000 monomers and more) with screened Coulomb interactions truncated after a certain number of bonds. This makes it possible to study chain-length dependence without “end effects” and to display excluded-volume effects. These correlation functions form the basis for a discussion of the conformational response to electrostatic interactions. In particular, they are related to the concept of electrostatic persistence length and the correlation functions illustrate the differences between different definitions of persistence length. To facilitate future discussions, we have identified four types of definitions and given them separate names: (1) projection length, which involves integration of the orientational correlation function; (2) orientational correlation length, which is the decay length of an exponential function; (3) bending coefficient, which is a length representing a bending force constant; and (4) crossover distance, which is the monomer–monomer distance at the boundary between a rodlike and a swollen behavior. Previous conclusions that the projection length obeys a power law at high salt concentrations, while the orientational correlation length does not, are confirmed. Furthermore, a power law is also found in the salt-free limit for the projection length corresponding to an infinite chain with a finite range of interactions. The two power laws make it possible to construct a universal curve that gives an almost quantitative description of the chain behavior.

Introduction

One of the most fundamental features of flexible polyelectrolytes is the conformational behavior caused by the electrostatic interactions, because many experimentally observed properties of polyelectrolyte solutions depend on it. It would be desirable to capture the general behavior in relatively simple terms (both conceptually and mathematically) as has been done for neutral polymers in, for example, the concepts of excluded volume interactions and scaling.^{1,2} However, the treatment of neutral polymers is simplified by the fact that the interactions are generally short-ranged, while electrostatic interactions are long-ranged. Still, Odijk³ and, independently, Skolnick and Fixman⁴ (OSF) found a simple power law for the electrostatic persistence length, $l_{p,e}$, in a model of a very stiff chain. For very long chains, the electrostatic persistence length was found to be proportional to κ^{-2} , where κ^{-1} is the Debye screening length. This behavior has been confirmed experimentally for rather stiff chains.^{5,6}

In contrast, experiments on flexible chains,^{7–10} as well as variational calculations^{11–14} and simulations^{15–18} have given $l_{p,e} \sim k^{-p}$ with $p \approx 1$. There are more than one definition of persistence length, however. They are equivalent for the wormlike chain model, but not for a charged polymer, as was shown recently.¹⁸ The difference is that the stiffening of a wormlike chain is only transmitted along the contour, while electrostatic interactions act through space. Another common definition gives no consistent power law and $p < 1$ for completely flexible chains.^{18–20} Furthermore, p grows toward the OSF limit, if the chains are made increas-

ingly stiff with the help of a bond angle potential.^{18,20} Transitions between $p = 1$ and OSF-like behavior have also been discussed theoretically by Barrat and Joanny¹² and by Ha and Thirumalai.^{13,14} Purely OSF-like behavior have been obtained variationally by Li and Witten²¹ and by Netz and Orland for the three-dimensional case (if the results are rescaled with the average bond length as the basic unit of length).²²

Liverpool and Stapper have argued that there should be no simple power law.^{23,24} This was based on an expression obtained from a field-theoretic renormalization group analysis. However, the applicability to three dimensions is questionable.²⁵ For example, a figure which appears to show simulation data in support of the theory,²³ was actually not plotted correctly. In reality, the expression does not reflect a universal behavior of the data as it should.

The picture might appear complex, but a part of it is a matter of bookkeeping. For polyelectrolytes, the different definitions of persistence length should be treated as different properties and it should always be made clear which of the properties is being discussed. The fact remains that a power law dependence on a parameter combining charge density and screening length is observed for one of the definitions, which means that there are fundamental and general relationships governing the behavior. An understanding of these relations should lead to both better and simpler descriptions of polyelectrolytes.

It has been suggested that the difference between the OSF behavior, $p = 2$, and the result $p = 1$ is due to so-called excluded volume effects,^{22,26} i.e., interactions between sections of the chain that are far apart in sequence but may get close in space occasionally, due to the chain bending back on itself. If the distance between the sections is on average much longer than

* To whom correspondence should be addressed.

[†] Lund University.

[‡] University of New South Wales.

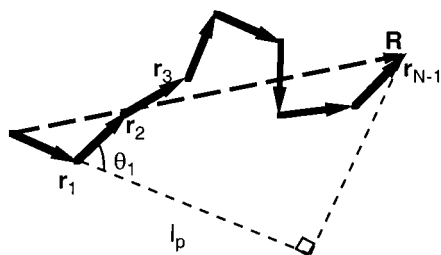


Figure 1. Freely jointed chain represented by the bond vectors \mathbf{r}_j . \mathbf{R} is the end-to-end vector.

the range of electrostatic interactions, there is no direct contribution to the chain stiffness, but the occasional interactions still affect the long-range orientational correlations.

To separate out the excluded volume effects, simulations of long chains, $N = 1000$ monomers and more, have been performed with the screened Coulomb potential truncated after $n - 1$ bonds; i.e., the N -mer is made up of overlapping subchains with n interacting monomers. This also makes it possible to study chain length dependences without end effects, since virtually all monomers find themselves at the middle of such a subchain; i.e., all monomers are equivalent.

The paper is outlined as follows: First, the basic concepts of persistence length are reviewed and a new terminology is introduced to separate the different properties. The details of the simulations are then described briefly, followed by the results. The first part of the results section discusses the orientational correlation function, which displays the conformational response to electrostatic interactions directly. It both reveals differences between different types of persistence length and illustrates electrostatic excluded volume effects. The latter part of the results section deals with power laws in both the high-salt and salt-free limits and their combination into a universal behavior. The paper ends with a summary.

Persistence Length

The concept of persistence length dictates that it should be a measure of stiffness, but exactly how this is measured is a matter of definition and there are plenty of definitions. It is possible to pick out four basic ones. Many other definitions are closely related to these and the four can be said to represent the principal definitions of four main groups. The first three are closely related to the orientational correlation function, while the fourth is expressed in terms of the distance correlation function. To distinguish the different definitions as different properties, we will give them separate names and symbols.

Definition 1: Projection Length, l_p , the Projection of the End-to-End Vector on the Direction of the First Bond. For a freely jointed chain with rigid bonds, we have

$$l_p = \frac{1}{b} \langle \mathbf{r}_1 \cdot \mathbf{R} \rangle = \frac{1}{b} \sum_{j=1}^{N-1} \langle \mathbf{r}_1 \cdot \mathbf{r}_j \rangle = b \sum_{k=0}^{N-2} \langle \cos \theta_k \rangle \quad (1)$$

where b is the bond length and $\langle \dots \rangle$ denotes an ensemble average. \mathbf{r}_j is a bond vector, \mathbf{R} is the end-to-end vector, N is the number of monomers (which makes $N - 1$ bonds), and θ_k is an angle between bond vectors separated by k bonds (see Figure 1).

For a continuous-chain model (space curve) the sum in eq 1 corresponds to an integral

$$l_p = \int_0^L C(s) ds \quad (2)$$

where $C(s) \equiv \langle \cos \theta(s) \rangle$ is the orientational correlation function, s is a contour distance and L is the contour length.

There is a point to keeping the commonly used symbol for persistence length, l_p , for the projection length. It has an interesting behavior for charged chains and it can be measured experimentally in dilute solutions (cf. below), which makes it worthwhile to study.

Definition 2: Orientational Correlation Length, l_{oc} , the Correlation Length of an Orientational Correlation Function with an Exponential Decay. The orientational correlation function of a freely rotating chain with rigid bonds and rigid bond angles can be described with an exponential function:²⁷

$$C_k \equiv \langle \cos \theta_k \rangle = \langle \cos \theta_1 \rangle^k = e^{-kb/l_{oc}} \quad (3)$$

The wormlike chain model,²⁸ which is the corresponding continuous chain, has an exponential correlation function by definition:

$$C(s) = e^{-s/l_{oc}} \quad (4)$$

For the sake of the following discussion, we introduce a more general exponential correlation function with a prefactor C_0 :

$$C(s) = C_0 e^{-s/l_{oc}} \quad (5)$$

This allows for a long-range exponential decay, while ignoring the true behavior at short length scales.

Inserting the two-parameter function into eq 2, gives $l_p = C_0 l_{oc}$ in the limit $L \rightarrow \infty$; i.e., definitions 1 and 2 are equivalent for an infinite chain if $C_0 = 1$, the value of C_0 for a true wormlike chain.

Definition 3: Bending Coefficient, l_{bc} , a Parameter That Specifies the Bending Energy. The total bending energy of a continuous chain can be specified as

$$U_{\text{bend}} = \frac{1}{2} k_B T l_{bc} \int_0^L \frac{1}{\rho^2(s')} ds' \quad (6)$$

where $\rho(s')$ is the radius of curvature at a point s' on the contour. k_B is Boltzmann's constant and T is the absolute temperature.

If this is the only potential affecting the chain conformations, averaging over the conformations leads to²⁹

$$C(s) = e^{-s/l_{bc}} \quad (7)$$

i.e., the correlation function of a wormlike chain (cf. definition 2).

Note also that, if the electrostatic energy, compared to a rigid-rod conformation, can be expressed in the same way, i.e., $\Delta u_{el}(s') \propto 1/\rho^2(s')$, the intrinsic bending coefficient $l_{bc,0}$ and the electrostatic bending coefficient $l_{bc,e}$ are additive; i.e., the total bending coefficient is $l_{bc} = l_{bc,0} + l_{bc,e}$.

Definition 3 has been used in variational calculations and it is also the starting point of OSF theory.

Definition 4: Crossover Distance, l_{cd} , the Monomer—Monomer Distance Corresponding to a Crossover between a Rodlike (Persistent) Behavior and an Excluded Volume (Swollen) Behavior. Starting with Kratky and Porod,²⁸ the concept of a crossover distance has been used as a means to obtain a persistence length from the form factor measured in scattering experiments, where it is observed as a crossover in k -space. It has been applied to correlation functions in real space by Barrat and Boyer¹⁶ and by Netz and Orland.²² We will follow Netz and Orland, who expressed the real-space definition more precisely.

If there is a region where the mean-square end-to-end distance grows linearly with the number of bonds and this goes over into a final long-range behavior where it grows with a swelling exponent ν , the distance correlation function in these two regions can be represented as

$$\langle R(k)^2 \rangle = \begin{cases} b_2 k^2 & k < k_p \\ b_\infty k^{2\nu} & k > k_p \end{cases} \quad (8)$$

where b_2 and b_∞ are constants for a given chain and

$$k_p = \left(\frac{b_\infty}{b_2} \right)^{1/(2-2\nu)} \quad (9)$$

is the persistent crossover scale, i.e., the number of bonds where an extrapolation of the two types of behavior gives the same mean-square end-to-end distance. The crossover distance is then

$$l_{cd} = \langle R(k_p)^2 \rangle^{1/2} = b_2^{1/2} k_p = b_\infty^{1/2} k_p^\nu \quad (10)$$

Given the two-parameter exponential orientational correlation function we have (cf. eq 15)

$$\langle R(s)^2 \rangle = \begin{cases} C_0 s^2 & s \rightarrow 0 \\ 2C_0 l_{oc} s & s \rightarrow \infty \end{cases} \quad (11)$$

i.e., $\nu = 1/2$ and $s_p = 2l_{oc}$, which gives $l_{cd} = 2l_{oc}\sqrt{C_0}$. In the discussion of the results, we will show that this can be seen as the Kuhn length of an underlying wormlike chain. A trivial factor of 2 can, of course, be introduced into the definition to make l_{cd} equivalent to the other definitions for a wormlike chain ($C_0 = 1$).

While the projection length is related to an integral over the orientational correlation length, the crossover distance is related to the square root of such an integral, hence the factor $\sqrt{C_0}$ and the behavior is expected to be intermediate between the projection length and the orientational correlation length.

As seen above, an exponential orientational correlation function represents a Gaussian-type long-range behavior with $\nu = 1/2$, while chains with screened Coulomb interactions are expected to become self-avoiding walks with a swelling exponent close to the Flory value $\nu = 3/5$. If a projection length is calculated from $\langle R^2 \rangle = 2l_p L$ (eq 16), a long chain would give $l_p \sim N^{2\nu-1}$; i.e., the projection length becomes size-dependent when $\nu \neq 1/2$. This will be discussed more in connection with the results.

Experimental Persistence Lengths (Projection Length and Crossover Distance). Experimentally, the persistence length is usually measured indirectly via the wormlike chain prediction for another quantity.

For example, light-scattering experiments measure the radius of gyration. This involves an integral over the orientational correlation function and the result is the projection length, i.e., the persistence length according to definition 1.

This can easily be shown. The radius of gyration, R_G , is given by

$$R_G^2 = \frac{2}{L^2} \int_0^L ds' (L-s') \int_0^{s'} ds (s-s') C(s) \quad (12)$$

and with the two-parameter exponential correlation function, $C(s) = C_0 e^{-s/l_{oc}}$, we have

$$R_G^2 = C_0 \left[\frac{l_{oc} L}{3} - l_{oc}^2 + 2 \frac{l_{oc}^3}{L} - 2 \frac{l_{oc}^4}{L^2} (1 - e^{-L/l_{oc}}) \right] \quad (13)$$

which for very long chains ($L \gg l_{oc}$) becomes

$$R_G^2 = \frac{C_0 l_{oc} L}{3} \quad (14)$$

The latter equation is the one often used to convert an experimentally determined radius of gyration to a persistence length^{6,8,9} and since a wormlike chain is generally assumed ($C_0 = 1$), the reported property is the projection length $l_p = C_0 l_{oc}$, although it may have been presented as the orientational correlation length.

A similar analysis for the mean-square end-to-end distance gives

$$\langle R^2 \rangle = 2 \int_0^L (L-s) C(s) ds = 2C_0 l_{oc} [L - l_{oc}(1 - e^{-L/l_{oc}})] \quad (15)$$

with the long-chain limit

$$\langle R^2 \rangle = 2C_0 l_{oc} L \quad (16)$$

Since the Kuhn length, l_K , is defined as $\langle R^2 \rangle = l_K L$, the projection length is the type of persistence length most closely related to it. For long chains, we have the usual result $l_K = 2l_p$.

In general, any definition that states that the persistence length is proportional to an integral over the orientational correlation function belongs to the same group as the projection length.

On the basis of the fact that a wormlike chain behaves like a rod at short distances and like a Gaussian chain at large contour separations (eq 11), Kratky and Porod indicated how to measure a persistence length from a crossover point between the two types of behavior in the form factor,²⁸ i.e., as a crossover distance. Applied to a chain obeying the two-parameter orientational correlation function, their analysis leads to $l_{cd} \propto \sqrt{C_0} l_{oc}$, as expected from the real-space definition above.

X-ray or neutron scattering is needed to probe the relevant length scales and these measurements are often performed above the overlap concentration to obtain sufficient scattering intensity and the crossover distance obtained at these polyelectrolyte concentrations is not representative of independent chains, which we focus on here. There are also practical problems pinning down the crossover point,³⁰ and an alternative is to fit scattering functions for wormlike chains.^{31,32}

When a nontrivial theoretical expression for a wormlike chain is fitted, it is less transparent which definition of persistence length is actually measured. It seems

reasonable to assume, however, that when properties depending on the entire chain are measured, a projection length is obtained, while experiments probing parts of the chain yield the persistence length of an underlying average chain. In the results we will show that the latter corresponds to a crossover distance, at least when the two-parameter correlation function is applicable.

OSF Theory (Bending Coefficient). In OSF theory, as in most simulations and theories for the persistence length, the electrostatic interactions are described by a screened Coulomb potential

$$u_{sc}(r) = \alpha^2 k_B T l_B \frac{e^{-\kappa r}}{r} \quad (17)$$

where α is the degree of ionization and $l_B = e^2 / (4\pi\epsilon_r\epsilon_0 k_B T)$ is the Bjerrum length, with e the elementary charge, ϵ_r the dielectric constant of the solution and ϵ_0 the permittivity of vacuum. When the polyelectrolyte is infinitely diluted and only monovalent ions are present, the Debye screening parameter is given by

$$\kappa^2 = 8\pi l_B N_A c_s \quad (18)$$

where c_s is the concentration of added 1:1 salt and N_A is Avogadro's number.

By calculation of the electrostatic contribution to first order for the bending of a rigid rod, the OSF model gives an electrostatic bending coefficient, which, following Odijk,³ can be expressed as

$$l_{bc,e} = \frac{(\alpha N)^2 l_B}{12} [3y^{-2} - 8y^{-3} + e^{-y}(y^{-1} + 5y^{-2} + 8y^{-3})] \quad (19)$$

with $y \equiv \kappa L$. For large y , this reduces to^{3,4}

$$l_{bc,e} = \frac{\alpha^2 l_B}{4\kappa^2 b^2} \quad (20)$$

In the salt-free case ($\kappa \rightarrow 0$), we have

$$l_{bc,e} = \frac{(\alpha N)^2 l_B}{72} \quad (21)$$

Previous Simulation Results for the Power Law Dependence of the Projection Length. When the only type of interaction is the screened Coulomb potential, eq 17, all average lengths, scaled by the bond length b , are functions of only three dimensionless numbers: $\xi_p = \alpha^2 l_B / b$ (coupling parameter), κb (screening parameter), and N (chain size).

It was shown previously that the electrostatic projection length for a freely jointed chain behaves as

$$\frac{l_{p,e}}{b} \sim \left(\frac{\xi_p}{\kappa b} \right)^p \quad (22)$$

where $p \approx 1.1$, when the screening length is shorter than the chain dimensions.¹⁸ The combination of α ($\xi_p^{1/2}$) and κ agrees with experiments.⁹ This is not very surprising, because it is a natural combination, since $\xi_p / (\kappa b)^2$ is the result (ignoring numerical constants) of a three-dimensional integral over the screened Coulomb potential and the same ratio appears also in theoretical results. Indeed, the long-chain OSF prediction can be written $l_{bc,e} / b = \xi_p / 4(\kappa b)^2$.

When the screening length is much larger than the size of the chain, the electrostatic interactions are essentially unscreened and both the projection length and the orientational correlation length are independent of κ .

Persistence Lengths Measured in the Present Simulations. We have organized persistence length into different properties, but there are still different ways to calculate each property, in particular the projection length.

In the present simulations, the interactions are truncated after n monomers, but at low salt concentrations there may still be significant correlations over the entire length of the chain; i.e., C_k has not decayed completely to zero for k values on the order of N . A finite sum, as in eq 1, would thus introduce a size dependence, while we prefer the projection length to be an intrinsic property of a chain with given n ; i.e., we want the result corresponding to an infinite chain, which is uniquely defined. Strictly speaking, it is also only in this limit that the projection length is given by the radius of gyration through eq 14, which is used experimentally, although it may be a good approximation when the projection length is small at high salt concentrations. There will still be a dependence on n , but when the sum is taken to infinity, the n dependence will only be governed by the interactions.

The simplest approach is to assume an exponential decay and fit $C_0 e^{k b / l_{oc}}$ to the orientational correlation function C_k (in practice through linear regression of $\ln C_k$ vs k) and integrate to infinity, yielding $l_p = C_0 l_{oc}$. The correlation length, l_{oc} , obtained this way represents long-range correlations, as can be seen from the results, although it may be something of a compromise when there are extensive excluded volume effects.

The results also show that, at high salt concentrations, the integral over the fitted exponential function neglects a contribution from the true correlation function at shorter contour separations. This contribution is taken care of in the direct summation of eq 1. If the correlation function has not decayed sufficiently at the end of the finite chain, the infinite chain result can be obtained by supplementing the sum of eq 1 with an integral over the tail of the fitted function.

We are interested in the response to electrostatic interactions and we should therefore separate out an electrostatic persistence length. It is generally assumed that the intrinsic and electrostatic persistence lengths are additive. This is true for the bending coefficient in the OSF model, but it is not obvious that it should hold for all definitions and models. The situation is simplified, however, by the fact that the simulations are based on freely jointed chains. The continuous-chain analogue is a completely uncorrelated chain; i.e., there is no intrinsic persistence length and the projection length and the orientational correlation length obtained by fitting an exponential correlation function have a purely electrostatic origin.

When using the direct summation, eq 1, there is a contribution from the finite bond length ($\cos \theta_0 = \cos 0 = 1$). For this case, we define an electrostatic projection length

$$l_{p,e} = \lim_{N \rightarrow \infty} b \sum_{k=0}^N \langle \cos \theta_k \rangle - b = \lim_{N \rightarrow \infty} b \sum_{k=1}^N \langle \cos \theta_k \rangle \quad (23)$$

which is zero for a freely jointed chain in the absence

of electrostatic interactions. The prime is used as a reminder that the result is based on the true correlation function and not just the fitted one. The limit as $N \rightarrow \infty$ is known to exist in the present case, because the correlations decay exponentially beyond the truncation of the interactions.

The sum is written as starting from an end, but in practice, we start from the center of the chain and stop 60 bonds from the end to avoid end effects. The fitted correlation function is used to extrapolate the summation to infinity, which is only needed at lower salt concentrations and for longer subchains. Likewise, the correlation function is also calculated with respect to the center of the chain.

Methods

A polyelectrolyte is represented as a freely jointed chain with rigid bonds of length b joining N monomers. Each monomer is a point charge and has a degree of ionization α , which is the same for all monomers. The polyelectrolyte is regarded as infinitely diluted and the charges interact via a screened Coulomb potential, eq 17, which is truncated after n monomers. Screening is considered to be the result of adding a 1:1 salt.

In most simulations $N = 1000$, but for $n = 320$ the chain length was 2000 at the salt concentrations 0–0.01 M for $b = 3$ Å and at 0–0.0001 M for $b = 12$ Å.

The simulations were performed in a canonical ensemble with the temperature $T = 298$ K and a dielectric constant, $\epsilon_r = 78.3$, corresponding to water at that temperature. Ensemble averages were obtained using the traditional Metropolis algorithm.³³ The conformational sampling was performed with a pivot algorithm,^{34,35} where trial conformations are obtained by dividing the chain into two parts around each bond in turn and rotating one part around the bond.³⁶ The rotation angle was picked randomly within a full circle.

Longer simulations were needed to get good statistics when the orientational correlation function was small, for example, at high salt concentrations. This is because the fluctuations depend on the length of the simulation and not the size of correlation function, which means that the relative error increases as the correlation function decreases. Not counting equilibration, the longest simulations lasted 2.5×10^8 Monte Carlo steps.

Results and Discussion

Correlation Functions. Figures 2 and 3 show logarithmic plots of the orientational correlation function for different subchain lengths and different salt concentrations. A wormlike chain would give a straight line passing through the origin, since its correlation function is a pure exponential with $C_0 = 1$. For the chains simulated here, an exponential behavior should develop at large separations along the contour, since there are no interactions beyond $n - 1$ bonds and long-range correlations can then only propagate through the chain.

Figure 2 shows that the exponential behavior, seen as a linear relationship, can be established at contour separations even shorter than the truncation length. At these lower salt concentrations, the stiffness of the chain, represented by either the projection length or the orientational correlation length, is longer than range of the interactions, given by κ^{-1} (see Table 1). With $n = 160$ and 320 the subchains have end-to-end distances longer than the screening length, while the projection length is longer than the end-to-end distance. Thus, the electrostatic interactions have decayed below significant levels before they are truncated and the chain stiffness prevents closer contacts between distant parts of a

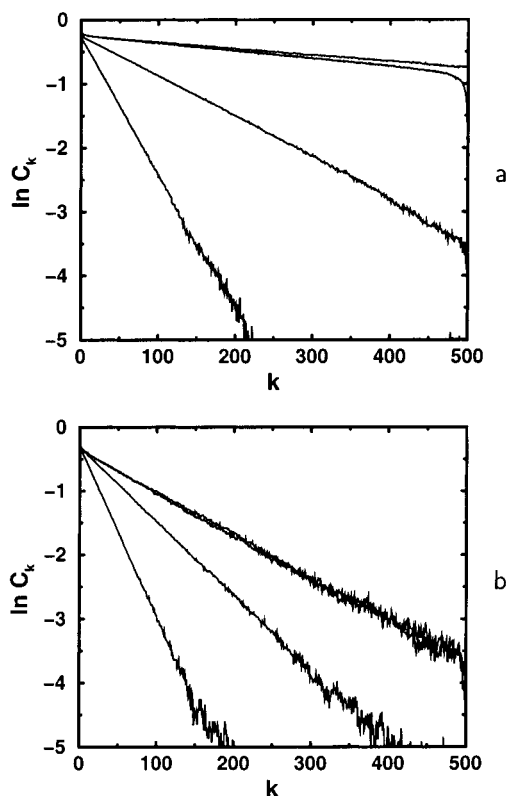


Figure 2. Orientational correlation functions for chains with subchain lengths $n = 320, 160, 40$, and 20 monomers (top to bottom) at two concentrations of added 1:1 salt: (a) 0.001 M and (b) 0.01 M. $b = 3$ Å, and $\alpha = 1$.

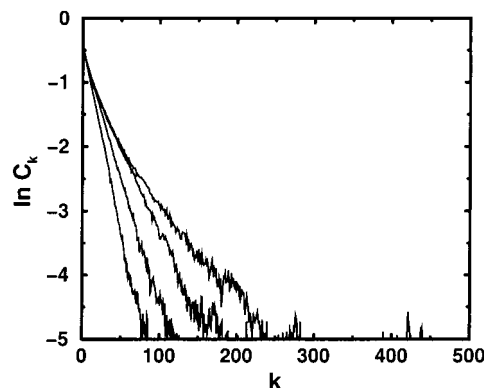


Figure 3. Orientational correlation functions for chains with subchain lengths $n = 320, 160, 40$, and 20 monomers (top to bottom) at 0.1 M salt. $b = 3$ Å, and $\alpha = 1$.

subchain. The correlation functions for $n = 160$ and 320 are therefore almost the same in Figure 2. In contrast, with $n = 20$ and 40 , the interactions have not decayed completely at the truncation length and the persistence length is reduced due to the reduced interactions.

Note that the intercept, $\ln C_0$, is not zero as it would be if the correlations only acted through the bonds. Thus, a prefactor $C_0 \neq 1$ is needed to fit even a correlation function that is almost entirely exponential. This may be interpreted as a part of the chain making up an effective bond, as in the blob model,^{37,38} or as the chain being coupled to a wormlike tension field.^{12,14}

It can also be expressed in the following way: On a global scale, the chain fluctuates around an average chain, which is wormlike with a correlation function $e^{-s/l_{av}}$. On a local scale, the freely jointed chain is far from wormlike, but each bond has an average projection

Table 1. Screening Lengths, Root-Mean-Square End-to-End Distances of Subchains and Persistence Lengths for the Cases Represented in Figures 2 and 3, Where $b = 3 \text{ \AA}$ and $\alpha = 1^a$

c_s/M	κ^{-1}	n	$\langle R(n)^2 \rangle^{1/2}$	$l_{p,e}$	$l_p = C_0 l_{oc}$	C_0	l_{oc}
0.001	96	20	47	105	106	0.75	140
		40	99	369	372	0.79	470
		160	410	1904	1904	0.79	2421
		320	803	2320	2326	0.78	2981
0.01	30	20	46	82	82	0.73	113
		40	93	187	188	0.73	258
		160	410	310	308	0.67	457
		320	595	315	316	0.71	445
0.1	10	20	40	35	34	0.68	51
		40	74	45	45	0.61	75
		160	210	59	57	0.50	114
		320	330	68	62	0.39	162

^a C_0 and l_{oc} have been obtained by fitting a general exponential function, $C_0 e^{-s/l_{oc}}$, to the orientational correlation functions, while $l_{p,e}$ is the result of a direct summation, which has been extrapolated with the help of the fitted function when necessary. The unit of length is \AA .

$b \langle \cos \phi \rangle = b \sqrt{C_0}$ on the underlying wormlike chain. This means that $\langle \mathbf{r}_i \cdot \mathbf{r}_j \rangle = b^2 \langle \cos \theta_{j-i} \rangle$ can also be written

$$\langle \mathbf{r}_i \cdot \mathbf{r}_j \rangle = (b \langle \cos \phi \rangle)^2 \langle \mathbf{t}_i \cdot \mathbf{t}_j \rangle = b^2 C_0 e^{-(j-i)b\sqrt{C_0}/l_{av}} \quad (24)$$

where \mathbf{t}_i is a unit vector for the tangential direction of the wormlike chain. Thus, the underlying chain has a contour length $L_{av} = (N-1)b\sqrt{C_0}$ and its orientational correlation length l_{av} is $l_{oc}\sqrt{C_0}$ in terms of the real chain. Note that the underlying chain is a wormlike chain with the same radius of gyration and mean-square end-to-end distance as the real chain (cf. eqs 13–16), which could have been used as a definition of an effective chain to obtain L_{av} and l_{av} directly.

This is closely related to the model of a wormlike tension field. There, the real chain is coupled locally to a tension of magnitude τ and with a direction varying along the chain on average like a wormlike chain, with an orientational correlation length l_{oc} . Since the orientational correlation length of the tension field is usually expressed with respect to a contour distance of the real chain,^{12,14} it corresponds to the real l_{oc} (as opposed to $l_{av} = l_{oc}\sqrt{C_0}$). From the above interpretation of the two-parameter model, one can see that the magnitude of the tension corresponds to $\tau = 3\sqrt{C_0}/b$. This is because a freely jointed chain with the ends fixed on the axis of a constant tension τ has an average end-to-end distance $\langle R \rangle = \tau(N-1)b^2/3$ when the extension is not too large, $\langle R \rangle \ll (N-1)b$.³⁹ Thus, each bond has an average projection $\langle R \rangle/(N-1) = \tau b^2/3 = b\sqrt{C_0}$ on the direction of the tension, where the last equality comes from identifying the tension field with an underlying wormlike chain.

Given the two-parameter exponential correlation function, the crossover distance is $l_{cd} = 2l_{oc}\sqrt{C_0} = 2l_{av}$ (see eq 11), and we see that l_{cd} is the Kuhn length of the underlying wormlike chain, since the Kuhn length is just twice the orientational correlation length of a true wormlike chain, when the chain is (infinitely) long.

When the persistence length is short compared to the length of the subchain, distant parts get a higher probability of being close and there is a contribution to the long-range correlations from the resulting pair interactions. This electrostatic excluded volume effect can clearly be seen in Figure 3. At high salt concentra-

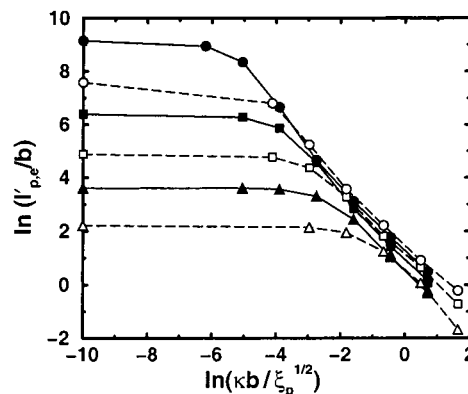


Figure 4. Projection length from direct summation (extrapolated when necessary). Data are shown for $\alpha = 1$ and bond lengths of 3 \AA (filled symbols/solid lines) and 12 \AA (open symbols/dashed lines) with interaction ranges of 20 monomers (triangles), 80 monomers (squares), and 320 monomers (circles). The points on the y-axis are for the salt-free case.

tions, the chains with different subchain lengths have the same behavior at low k . The excluded volume interactions decrease the decay of $\ln C_k$ vs k gradually as k increases, until the truncation takes effect and the relationship becomes linear.

It is clear that the two-parameter model with an exponential decay works best as a description of the orientational correlation function at low salt concentrations when excluded-volume effects are small.

The results illustrate the fact that the projection length and the orientational correlation length are distinctly different properties when applied to polyelectrolytes. If an exponential function is fitted to the correlation function, the orientational correlation length is the same for a chain that has a consistent decay length, due to interactions within sequences comparable to the screening length, as for a chain that happens to have the same decay length for large k at a higher salt concentration, due to excluded volume interactions. The projection length, on the other hand, takes into account the greater flexibility (lower values of C_k) at the higher salt concentration and gives a lower value in the latter case.

The difference is a result of the nonwormlike behavior of polyelectrolytes, seen in $C_0 \neq 1$ for the fitted correlation function, even when the decay is exponential, and in the nonexponential behavior at high salt concentrations, the excluded volume effect. There is no fundamental difference between these two effects, however. They both express the fact that electrostatic interactions act through space, as opposed to a simple propagation through bonds. Excluded volume interactions of neutral polymers also act through space, but the electrostatic interactions are stronger and more long-ranged. The resulting conformational response is therefore much more pronounced in polyelectrolytes.

Power Law: High-Salt Limit. Previous simulations have shown that a finite-chain version of the projection length (corresponding to direct summation without extrapolation) obeys $l_{p,e}/b \sim (\xi_p^{1/2}/\kappa b)^p$, where $p \approx 1.1$, when the screening length is shorter than the chain dimensions,¹⁸ while the orientational correlation length lacks a consistent power law.^{18–20}

These general conclusions are also illustrated by Figures 4 and 5 obtained from the simulations with truncated interactions (the salt concentration increases from left to right in the figures). A reason the projection

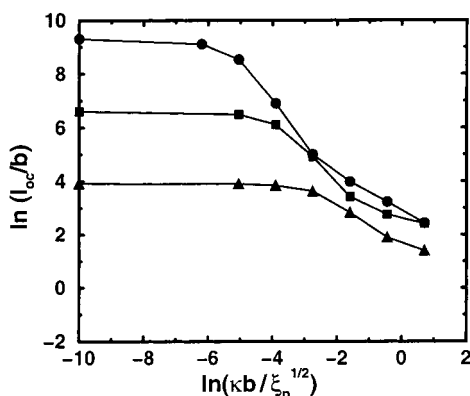


Figure 5. Orientational correlation length. Data are shown for a bond length of 3 Å with the same symbols as in Figure 4.

length depends on a specific parameter combination in a power law, while the orientational correlation length does not, may be that the integral over the correlation function takes all length scales into account and thus includes the balance between conformational and electrostatic contributions to the free energy. Information is lost, however, if only the correlation length l_{oc} is used.

Figure 4 shows the behavior of the projection length calculated as for an infinite chain through the extrapolated direct summation. The exponent p is about 1.2 at high salt concentrations. The higher value of the exponent, compared to the previous result, is due to the extrapolation to infinity. If the projection length is calculated over just the length of a subchain, the exponent is about 1.1 as before. Another difference is that end effects are suppressed in the present approach with subchains within longer chains. The projection length has increased roughly 10% compared to the previous case, where the chain ends were included in the results. This does not affect the exponent to any significant degree, however.

For length scales $\kappa b k \gg 1$, the behavior of a fully interacting chain is expected to be dominated by excluded volume interactions and the chain should behave as a self-avoiding walk, leading to a size-dependent projection length as explained above (see definition 4). The truncation of the interactions in the simulations turns the long-range behavior into that of a random walk and the orientational correlation function becomes truly exponential, but for $\kappa b n \gg 1$ there are excluded volume interactions within the subchains and we see a dependence on n in Figure 4.

It is probably easier to visualize the origin of the n dependence through the correlation function, remembering that the projection length is an integral over it. At high salt concentrations and with given values of κb and ξ_p , chains with different n have the same correlation function at contour separations k shorter than the truncation n . Beyond the truncation, however, C_k is smaller for shorter subchains with $n < k$ than for longer ones (cf. Figure 3). Thus, the integral will be smaller for smaller n . When fitting the two-parameter exponential function, some of these effects are reflected in C_0 and l_{oc} , but the fitting procedure is a compromise between the range of k -values where the correlation function is the same for differing n and the range where it is not, while the direct summation takes the difference into account completely, being the true integral. The result is that the dependence of the subchain length based on the fitted function $l_p \sim n^{0.1}$ is weaker than for

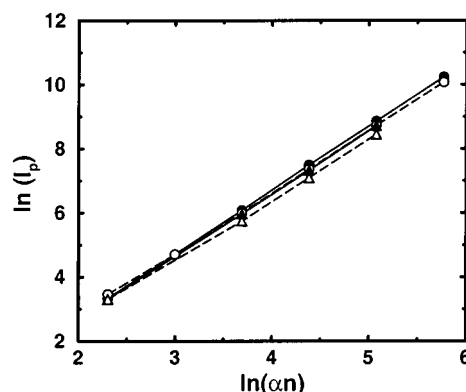


Figure 6. Projection length in the salt-free limit. Data are shown for bond lengths of 3 Å (filled symbols/solid lines) and 12 Å (open symbols/dashed lines) with $\alpha = 0.5$ (triangles) and 1 (circles). The interaction ranges are 10–320 monomers.

the direct summation $l_{p,e} \sim n^{0.3}$. A rough estimate using $\langle R(n)^2 \rangle \approx 2l_p b(n-1)$ and $\langle R(n)^2 \rangle \sim n^{2\nu}$ with the Flory value $\nu = 3/5$ would give $l_p \sim n^{0.2}$.

For the direct summation, the high-salt behavior can be summarized as

$$\frac{l_{p,e}}{b} \approx B \left(\frac{\xi_p^{1/2}}{\kappa b} \right)^{1.2} n^{0.3} \quad (25)$$

with the numerical constant $B \approx 0.8$.

Power Law: Salt-Free Limit. The Odijk expression of OSF theory, eq 19, predicts that $l_{oc,e} \sim (\alpha n)^2$ in the salt-free limit (eq 21). Figure 6 shows how the projection length depends on αn . This combination does indeed capture a common behavior of the different chains and the slope is about 1.9. The orientational correlation length gives similar slopes, but there is not a single, universal curve. In terms of the dimensionless variables and assuming a quadratic dependence, the limiting behavior at low salt concentrations is

$$\frac{l_p}{b} \approx A \xi_p n^2 \quad (26)$$

with the numerical constant $A \approx 0.04$.

It should be remembered, however, that OSF theory predicts the electrostatic bending coefficient, which is intrinsically different from both the projection length and the orientational correlation length for a freely jointed chain, because the chain is not wormlike. Even at low salt concentrations, where the electrostatic interactions give the freely jointed chain a long-range stiffness and the correlation function for a chain with truncated interactions has an exponential decay that starts at relatively short contour separations, the short-range correlations are still not wormlike. Naively, one might expect the OSF theory to be applicable to a rescaled, underlying wormlike chain, i.e., the type of the model discussed in connection with eq 24. OSF theory should then give $l_{oc}\sqrt{C_0}$, at least in the salt-free limit, but this appears not to be the case. Instead the qualitative behavior of the Odijk result in this limit is shared with $l_p = l_{oc}C_0$.

OSF theory calculates the energy difference between a rigid rod and a bent rod to first order. A projection of the charges onto an underlying, wormlike chain will not give the same energy as the true charge distribution. The connection freely jointed chain—average wormlike chain—OSF model is therefore in a sense broken. The

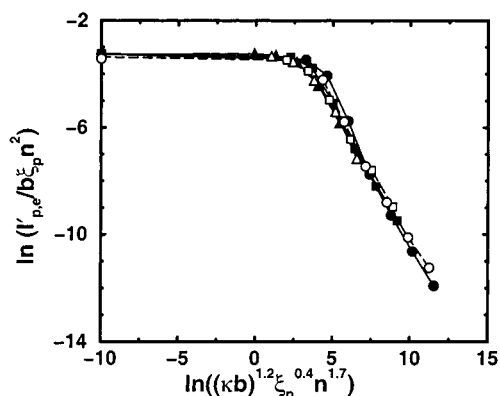


Figure 7. Universal behavior of the projection length from direct summation (extrapolated when necessary). The data are the same as in Figure 4.

integral over the correlation function, which gives l_p , may better represent the balance between electrostatic interactions and conformational freedom and, being a balance, could be more closely related to the electrostatic energy calculated in OSF theory. More detailed studies are needed to fully establish the connections and differences between the different types of persistence length.

Universal Behavior. Given the power laws in the two limits, no salt and high salt, the data can be collected into a universal curve, as shown in Figure 7. The exponents in the parameter on the x -axis have been chosen to produce a slope of -1 at high salt concentrations. In terms of this parameter, the crossover point, where the two limits would predict the same electrostatic projection length, $l_{p,e}$, is $(\kappa b)^{1.2} \xi_p^{0.4} n^{1.7} \approx 20$ ($\ln 20 \approx 3.0$). The empirical result can be summarized as

$$\frac{l_{p,e}}{b} \approx 0.04 \xi_p n^2 g(0.05 \xi_p^{0.4} (\kappa b)^{1.2} n^{1.7}) \quad (27)$$

where $g(x) = 1$ for small x and $g(x) = 1/x$ for large x , with a crossover at $x \approx 1$.

The figure reveals that, in the crossover region from the low-salt to the high-salt behavior, there is a tendency for the slope to increase as n and ξ_p increase. In fact, for $n = 320$ and $b = 3$ Å, the exponent p of $l_p/b \sim (\xi_p^{1/2}/\kappa b)^p$ is even slightly larger in the crossover region than in the final, high-salt part. The differing slopes are a result of the infinite chain extrapolation. For example, if $l_{p,e}/b$ is obtained by summing the correlation function up to just n , chains with different n show the same behavior in the crossover region. The extrapolation more fully accounts for the larger total interaction and stronger stiffening at larger n .

The excluded volume interactions have not yet been allowed to play a significant role in the crossover region and the differing slopes may indicate that very long chains, in the absence of excluded volume effects, could display a behavior closer to the OSF prediction, as discussed explicitly by Odijk and Houwaart²⁶ and by Netz and Orland.²² In fact, the results suggest that the Odijk expression, eq 19, is qualitatively correct up to a point where excluded volume interactions become significant. Further investigations are needed to establish this properly and confirm it for longer chains. In any case, it is clear that excluded volume effects make significant contributions to the projection length at the highest salt concentrations and, thus, affect the observed behavior.

Conclusions

Polyelectrolytes are not generally wormlike in the sense that the orientational correlation function follows a single, exponential decay at all length scales, although parts of the correlation function may behave exponentially. The difference is that electrostatic interactions are long-ranged and act through space, while the wormlike chain model is based on correlations that propagate only through the chain itself. One consequence of this is that various definitions of persistence length are no longer equivalent, but represent different properties. Any discussion about persistence length in the context of polyelectrolytes must therefore specify the definition used. We have identified four definitions and given the corresponding properties separate names: (1) projection length, which involves integration of the orientational correlation function; (2) orientational correlation length, which is the decay length of a (fitted) exponential function; (3) bending coefficient, which is a length representing a bending force constant; (4) and crossover distance, which is the monomer–monomer distance at the boundary between a rodlike and a swollen behavior.

The nonwormlike character of polyelectrolytes, in particular, if they are modeled as freely jointed chains, is evident from the orientational correlation function. At low salt concentrations and with interactions truncated after a certain number of bonds, most of the correlation can be described with an exponential function, but the prefactor of the exponential function is not 1, as required for the wormlike chain model. This is caused by the most short-range correlations, which have a different behavior. A direct consequence is the difference between the projection length and orientational correlation length.

At high salt concentrations, the correlation function decays slower than exponentially, because of increased chain flexibility and more frequent contacts between distant parts of the chain. This is often referred to as electrostatic excluded volume effects. The model with truncated interactions explicitly shows how the excluded volume effects affect the long-range correlations. Within the truncation, the short-range correlations are the same for different truncation lengths, while the decay turns exponential after the truncation and a difference is seen in the long-range correlations.

For an infinite chain where interactions are limited to subchains of length n , the orientational correlation length does not show consistent power laws in any range of salt concentrations, while the electrostatic projection length does both in the salt-free limit and at high salt concentrations. An almost quantitative description of the chain behavior can be given through the projection length by combining the two power laws into a universal curve.

Acknowledgment. This work was supported by the Swedish Natural Science Research Council. It was also greatly helped by permission to use the central LUNARC computer resource in Lund, Sweden.

References and Notes

- (1) Yamakawa, H. *Modern Theory of Polymer Solutions*; Harper and Row: New York, 1971.
- (2) de Gennes, P.-G. *Scaling Concepts in Polymer Physics*; Cornell University Press: Ithaca, NY, 1979.
- (3) Odijk, T. *J. Polym. Sci., Polym. Phys. Ed.* **1977**, *15*, 477–483.

- (4) Skolnick, J.; Fixman, M. *Macromolecules* **1977**, *10*, 944–948.
- (5) Maret, G.; Weill, G. *Biopolymers* **1983**, *22*, 2727–2744.
- (6) Mattoussi, H.; O'Donohue, S.; Karasz, F. E. *Macromolecules* **1992**, *25*, 743–749.
- (7) Tricot, M. *Macromolecules* **1984**, *17*, 1698–1704.
- (8) Ghosh, S.; Li, X.; Reed, C. E.; Reed, W. F. *Biopolymers* **1990**, *30*, 1101–1112.
- (9) Reed, W. F.; Ghosh, S.; Medjahdi, G.; Francois, J. *Macromolecules* **1991**, *24*, 6189–6198.
- (10) Degiorgio, V.; Mantegazza, F.; Piazza, R. *Europhys. Lett.* **1991**, *15*, 75–80.
- (11) Schmidt, M. *Macromolecules* **1991**, *24*, 5361–5364.
- (12) Barrat, J.-L.; Joanny, J.-F. *Europhys. Lett.* **1993**, *24*, 333–338.
- (13) Ha, B.-Y.; Thirumalai, D. *Macromolecules* **1995**, *28*, 577–581.
- (14) Ha, B.-Y.; Thirumalai, D. *J. Chem. Phys.* **1999**, *110*, 7533–7541.
- (15) Reed, C. E.; Reed, W. F. *J. Chem. Phys.* **1991**, *94*, 8479–8486.
- (16) Barrat, J.-L.; Boyer, D. *J. Phys. II* **1993**, *3*, 343–356.
- (17) Seidel, C. *Ber. Bunsen-Ges. Phys. Chem.* **1996**, *100*, 757–763.
- (18) Ullner, M.; Jönsson, B.; Peterson, C.; Sommelius, O.; Söderberg, B. *J. Chem. Phys.* **1997**, *107*, 1279–1287.
- (19) Micka, U.; Kremer, K. *Phys. Rev. E* **1996**, *54*, 2653–2662.
- (20) Micka, U.; Kremer, K. *Europhys. Lett.* **1997**, *38*, 279–284.
- (21) Li, H.; Witten, T. A. *Macromolecules* **1995**, *28*, 5921–5927.
- (22) Netz, R. R.; Orland, H. *Eur. Phys. J. B* **1999**, *8*, 81–98.
- (23) Liverpool, T. B.; Stapper, M. *Europhys. Lett.* **1997**, *40*, 485–490.
- (24) Liverpool, T. B.; Stapper, M. *Eur. Phys. J. E* **2001**, *5*, 359–375.
- (25) Ullner, M. Submitted for publication.
- (26) Odijk, T.; Houwaart, A. C. *J. Polym. Sci., Polym. Phys. Ed.* **1978**, *16*, 627–639.
- (27) Grosberg, A. Y.; Khokhlov, A. R. *Statistical Physics of Macromolecules*; AIP Press: New York, 1994; p 7.
- (28) Kratky, O.; Porod, G. *Recl. Trav. Chim. Pays-Bas* **1949**, *68*, 1106–1122.
- (29) Saitô, N.; Takahashi, K.; Yunoki, Y. *J. Phys. Soc. Jpn.* **1967**, *22*, 219–226.
- (30) Förster, S.; Schmidt, M. *Adv. Polym. Sci.* **1995**, *20*, 51–133.
- (31) Kirste, R. G.; Oberthür, R. C. In *Small-Angle X-ray Scattering*; Glatter, O., Kratky, O., Eds.; Academic Press: London, 1982; p 387–431.
- (32) Nierlich, M.; Boue, F.; Lapp, A.; Oberthür, R. *Colloid. Polym. Sci.* **1985**, *263*, 955–964.
- (33) Metropolis, N. A.; Rosenbluth, A. W.; Rosenbluth, M. N.; Teller, A.; Teller, E. *J. Chem. Phys.* **1953**, *21*, 1087–1097.
- (34) Lal, M. *Mol. Phys.* **1969**, *17*, 57–64.
- (35) Madras, N.; Sokal, A. D. *J. Stat. Phys.* **1988**, *50*, 109–186.
- (36) Ullner, M.; Jönsson, B.; Söderberg, B.; Peterson, C. *J. Chem. Phys.* **1996**, *104*, 3048–3057.
- (37) de Gennes, P. G.; Pincus, P.; Velasco, R. M.; Brochard, F. *J. Phys.* **1976**, *37*, 1461–1473.
- (38) Khokhlov, A. R.; Khachaturian, K. A. *Polymer* **1982**, *23*, 1742–1750.
- (39) Hill, T. L. *An Introduction to Statistical Thermodynamics*; Dover Publications: New York, 1986; p 218.

MA010863S